Desalination and Water Treatment
www.deswater.com
doi: 10.1080/19443994.2014.950988

56 (2015) 1610–1621
November

Taylor & Francis
Taylor & Francis Group

Synthesis of poly (styrene-divinyl benzene) magnetic porous adsorbents prepared by sulfonation for the adsorption of 2,4-dichlorophenol and 2,4,6-trichlorophenol from aqueous solutions

Ping Yu[a,b], Qilong Sun[c], Jianfeng Li[d], Jianming Pan[a], Zhenjiang Tan[b,*], Yongsheng Yan[a,*]

[a]*School of Chemistry and Chemical Engineering, Jiangsu University, 301 Xuefu Road, Zhenjiang 212013, China, Tel. +86 13843418813; email: jlsdyp@126.com (P. Yu), Tel. +86 15952850631; email: pjm@126.cn (J. Pan), Tel. +86 13952922917; email: yys@ujs.edu.cn (Y. Yan)*
[b]*School of Computer Science, Jilin Normal University, 1301 Haifeng Street, Siping 136000, China, Tel. +86 13944400585; Fax: +86-0434-3291953; email: jsdxtzj@126.com (Z. Tan)*
[c]*School of Management, Jilin Normal University, 1301 Haifeng Street, Siping 136000, China, Tel. +86 15694348877; email: 30880142@qq.com (Q. Sun)*
[d]*School of Foreign Language, Jilin Normal University, 1301 Haifeng Street, Siping 136000, China, Tel. +13500966226; email: 22043776@qq.com (J. Li)*

Received 18 November 2013; Accepted 13 July 2014

ABSTRACT

Poly(styrene-divinyl benzene) (St-DVB) magnetic porous microspheres were prepared by sulfonation for the adsorption of 2,4-dichlorophenol(2,4-DCP) and 2,4,6-trichlorophenol (2,4,6-TCP) from aqueous solution. The as-prepared microspheres were characterized by FT-IR, XRD, SEM, TGA, VSM, and N_2 adsorption–desorption techniques, showing that the as-prepared microspheres were porous and had good magnetism (Ms = 40 emu g^{-1}). The adsorption performance of St-DVB magnetic porous microspheres were investigated by batch mode adsorption experiments with respect to pH, temperature, initial concentration, and contact time. The St-DVB magnetic porous microspheres were sensitive to pH. The equilibrium data was better fitted to the Langmuir isotherm model than the Freundlich model. The kinetics experimental data was well fitted to the pseudo-second-order model. The thermodynamic parameters were calculated by the Gibbs free energy function, revealing that the adsorption process was spontaneous and endothermic. Furthermore, the St-DVB magnetic porous microspheres had good recycling performance.

Keywords: Suspension polymerization; Sulfonation; Magnetic porous adsorbent; 2,4-Didichlorophenol; 2,4,6-Trichlorophenol; Adsorption

1. Introduction

Chlorophenols are important raw materials in the synthesis of dye, pesticide, and pharmaceuticals [1,2]. However, at the same time, chlorophenols are one of the most common organic pollutants, which have been listed as priority pollutants by Environmental Protection Agency (EPA) [3]. Wastewater containing chlorophenols do great harm to human body and aquatic organisms [4]. According to EPA, permissible

*Corresponding authors.

level of chlorophenols concentration in wastewater is 0.1 mg L^{-1}. The World Health Organization sets a limit of chlorophenols concentration as 0.001 mg L^{-1} in potable water [5]. In these cases, effective removal of chlorophenols from aquatic environment is of great importance in environmental protection.

Various techniques and methods, such as photocatalytic degradation [6], chemical oxidation [7], biological degradation [8], solvent extraction [9], membrane separation [10], and adsorption [11], have been studied and used to deal with the chlorophenol-contained wastewater. Among these methods, adsorption is found to be the most effective treatment method due to its high efficiency, high selectivity, easy handling, and easy regeneration [2]. Activated carbon is the most common adsorbent used in the removal of chlorophenols from wastewater. But the activated carbon is of high cost due to hard regeneration [12]. It is significant to develop an alternative adsorbent with high adsorption capacity and easy regeneration.

In recent years, porous polymer adsorbents have been attracted much attention due to their low cost, low density, high porosity, simple handling, and easy functionalization. A variety of porous polymer adsorbents have been synthesized and widely applied to the removal of chlorophenols from aqueous solutions. The porous polymer microspheres are commonly prepared by the emulsion polymerization, bulk polymerization, suspension polymerization, and dispersion polymerization. Among these methods, suspension polymerization has been regarded as the most efficient and simple method, giving highly pure products with porosity, large adsorption capacity, and high-specific surface area. Various types of adsorbents, such as vinyl acetate/methyl methacrylate [13], glycidyl methacrylate [14], and vinylphosphonic acid/methacrylic acid [15] were prepared by the suspension polymerization method. The conventional adsorbents have drawbacks of tedious centrifugation or filtration in separation process, which can be well addressed by magnetic adsorbents [16]. However, most of the magnetic adsorbent materials suffer the drawbacks of the uneven distribution of iron oxide magnetic nanoparticles. Recently, magnetic porous adsorbents prepared by sulfonation were found to show well-distribution of magnetic iron oxide [17,18]. For example, sulfonated polystyrene divinyl benzene polymers were conducive to form a uniform distribution of magnetic porous particles [19].

In the present work, an alternative method was developed to synthesize magnetic porous polymer microspheres. Firstly, styrene-divinyl benzene (St-DVB) porous microspheres were prepared by the suspension polymerization. Then, the as-prepared porous microspheres were coated with sulfonic acid group by sulfonation with sulfuric acid as surface modification agent. After several times of ion exchange and oxidation process, magnetic porous microspheres were obtained. The resulting magnetic porous polymer microspheres were characterized by FT-IR, XRD, SEM, TGA, and N_2 adsorption–desorption techniques. 2,4-Dichlorophenol (2,4-DCP) and 2,4,6-trichlorophenol (2,4,6-TCP) were selected as two typical phenolic pollutants to evaluate the adsorption capacity of the adsorbents. The adsorption properties such as equilibrium isotherm, thermodynamics, and kinetics performance were investigated through the batch mode adsorption experiments.

2. Experimental

2.1. Materials

2,4-Dichlorophenol (2,4-DCP) and 2,4,6-trichlorophenol (2,4,6-TCP) were purchased from the Tianda Chemical Reagent Factory (Tianjin, China). Styrene (St), toluene, sodium chloride, methylene dichloride, and methyl alcohol were supplied by Sinopharm Chemical Reagent Co., Ltd (Shanghai, China). Azodiisobutyronitrile (AIBN), Divinyl benzene (DVB), and cyclohexanol were obtained from Aladdin reagent Co., Ltd (Shanghai, China). Sulfuric acid (98%), hydrogen peroxide, ferrous chloride tetrahydrate and hydroxide were purchased from Shanghai Zhongshi Chemical Reagent Co., Ltd (Yangzhou, China). Deionized ultrapure water was purified with a Purelab Ultra (Organo, Tokyo, Japan). All other chemicals used were of analytical grade and obtained commercially.

2.2. Preparation of St-DVB porous microspheres

The synthesis process of St-DVB porous microspheres was followed by a modified suspension polymerization [20]. The process steps include: first, sodium chloride (1.5 g) was dissolved into 75 mL of deionized ultrapure water. Then, hydroxyethyl cellulose (0.9 g) was added to the above solvent with stirring at room temperature for 15 min to form aqueous phase. The organic phase was composed of monomer (5 mL styrene and 7.5 mL divinylbenzene), initiator (0.25 g azodiisobutyronitrile), and porogen (4.2 mL toluene and 6.25 mL cyclohexanol). After fully stirred, a stable emulsion was obtained by mixing the aqueous phase and organic phase together under ultrasonic treatment for 30 min. Then the emulsion was transferred into a 250 mL three-necked flask equipped with a condenser, N_2 inlet, and magnetically stirred for 1.0 h under nitrogen gas protection. Thereafter, the temperature was increased to 70℃ and the reaction was allowed to proceed with a stirring rate of

800 rpm min^{-1} for 24 h. Subsequently, the obtained St-DVB porous microspheres were washed with ethanol, acetone, and deionized ultrapure water for three times in order to remove water-soluble impurities. Finally, the microspheres were extracted with methylene dichloride in a Soxhlet extractor to remove organic impurities, which is followed by washing with deionized ultrapure water and methanol for three times; the purified St-DVB porous microspheres were dried under vacuum for 24 h. [21]

2.3. Preparation of St-DVB magnetic porous polymer microspheres

The St-DVB magnetic porous microspheres were prepared as follows:

(1) The surface modification process: Two gram of St-DVB porous microspheres and 25.0 g of sulfuric acid (98%) were added into a 50 mL three-necked flask, and the mixture was stirred at 50°C for 5.0 h. The obtained yellow viscous liquid was washed with acetone for three times. Sulfonated polystyrene microspheres were collected and dried at 80°C under vacuum; the quality of the products obtained was 1.5 g.
(2) Ion exchange process: 1.5 g sulfonated polystyrene microspheres and 65.0 mL ferrous chloride tetrahydrate (1.0 mmol) were added into a three-necked flask, and then the mixture was stirred at room temperature for 24 h to ensure adequately ion exchange.
(3) Oxidation process: After the ion exchange, the obtained microspheres were washed with deionized ultrapure water and filtered with sand core funnel to remove the organic impurities. Thereafter, the microspheres were transferred into another 250 mL three-necked flask, and then 40 mL deionized ultrapure water and 40 mL sodium hydroxide (3.75 mol L^{-1}) solution were also added into the flask. The mixture was stirred at 200 rpm min^{-1} and the temperature was increased to 60°C. Subsequently, 20 mL of hydrogen peroxide (30 wt%) solution was added dropwise under vigorous stirring. After 15 min, the flask was sealed and the reaction was maintained at 60°C for 1.5 h. Finally, the resultant microspheres were washed with deionized ultrapure water in an ultrasonic cleaning machine to neutral and then dried at 70°C under vacuum for 24 h.

In this work, in order to improve the mass fraction of magnetic nanoparticles in the microspheres, the ion exchange and oxidation process were repeated for three times. The resulting magnetic porous polymer microspheres were obtained.

2.4. Instruments and apparatus

The shape and surface morphology of the St-DVB magnetic porous microspheres were carried out on a scanning electron microscope (FE-SEM, S-4800). Fourier transmission Infrared spectra (4,000–400 cm^{-1}) were recorded on a Nicolet NEXUS-470 FT-IR apparatus (USA). Magnetic measurements were carried out using a VSM (7,300, Lakeshore) under a magnetic field. Raman spectra were recorded in the range of 200–800 cm^{-1} using a WITEC Spectra Pro 2300I spectrometer equipped with an Ar-ion laser, which provided a laser beam of 514 nm wavelength [22]. The thermo gravimetric analysis and differential scanning calorimetric were carried out using a DSC/DTA-TG (STA 449C Jupiter, Netzsch, Germany) under a nitrogen atmosphere up to 800°C with a heating rate of 5.0°C min^{-1}. The photographs of the magnetic separation were obtained by Canon IXUS125 HS. Elemental analysis was carried out on an elemental analyzer (Elementary, Hanau, Germany). The identification of crystalline phase was performed using a Rigaku D/max-γB X-ray diffractometer (XRD) with monochromatized Cu Kα radiation over the 2θ range of 20–80° at a scanning rate of 5.0° min^{-1}. High performance liquid chromatography (HPLC, Shimadzu, Japan) is equipped with a UV detector for the detection of phenolic compounds (2,4-DCP and 2,4,6-TCP). The injection loop volume was 20 μL, and the mobile phase consisted of deionized ultrapure water and methanol with a volume ratio of 70:30 for 2,4-DCP and 72:28 for 2,4,6-TCP, respectively. The flow rate of the mobile phase was 1.0 mL min^{-1} [23].

2.5. Adsorption studies

The experimental environment parameters, such as pH, temperature, initial concentration, and contact time on the adsorptive removal of 2,4-DCP and 2,4,6-TCP were studied by a batch mode of experiments.

To determine the effect of solution pH on the adsorptive removal of 2,4-DCP and 2,4,6-TCP from aqueous solution, 10 mg of St-DVB microspheres were dispersed in 10 mL of solution containing 100 mg L^{-1} 2,4-DCP or 2,4,6-TCP. The solution initial pH value was adjusted from 2.0 to 8.0 by using 1 mol L^{-1} HCl and $NH_3{\cdot}H_2O$ solutions. The mixture solutions were stewed in thermostatic water bath at 25°C for 12 h.

Equilibrium experiments were performed by contacting 10 mg St-DVB microspheres with 10 mL of

2,4-DCP (pH = 2.0) or 2,4,6-TCP (pH = 3.0) solutions with various initial concentrations from 10 to 400 mg L^{-1}. The mixture solutions were stewed in thermostatic water bath at 25°C for 12 h.

Adsorption kinetics experiments were studied over an reaction time that varied from 10 to 480 min. Ten milligram of St-DVB microspheres were added into 10 mL of solution containing 100 mg L^{-1} 2,4-DCP or 2,4,6-TCP which the solution pH of 2.0 for 2,4-DCP and 3.0 for 2,4,6-TCP, respectively. The temperature was kept at 25°C in a thermostatic water bath.

After the desired time, St-DVB magnetic porous microspheres were separated from the solutions by an external magnetic field. Then the residual concentration of 2,4-DCP and 2,4,6-TCP in aqueous solutions were determined with a UV spectrophotometer. The maximum absorbance values were set at 282 nm for 2,4-DCP and 290 nm for 2,4,6-TCP, respectively.

Moreover, the equilibrium adsorption capacity (Q_e, mg g^{-1}) was calculated according to Eq. (1):

$$Q_e = \frac{(C_0 - C_e)V}{W} \quad (1)$$

where C_0 (mg L^{-1}) is the initial concentration, C_e (mg L^{-1}) is the equilibrium concentration of adsorbate (2,4-DCP or 2,4,6-TCP), V(L) is the solution volume, and W (g) is the weight of the adsorbent.

2.6. Regeneration

Regeneration study of the St-DVB magnetic porous microspheres was conducted by using methanol/acetic acid (90:10, v/v) solution as desorption eluent. Adsorption process was first followed by the previous steps. Then the St-DVB magnetic porous microspheres with adsorbed 2,4-DCP and 2,4,6-TCP were separated rapidly from the solutions by an external magnetic field, and a UV spectrophotometer was used to analyze the remnant concentrations of 2,4-DCP and 2,4,6-TCP. Subsequently, the adsorbents were washed with 5 mL desorption eluent, after separation and vacuum drying for 12 h, microspheres were once again added into 2,4-DCP and 2,4,6-TCP solutions. To investigate the regenerability of the adsorbents, the adsorption and desorption cycles were repeated for three times.

3. Result

3.1. Characterization of St-DVB

The FT-IR spectra of the St-DVB porous microspheres and St-DVB magnetic porous microspheres are shown in Fig. 1. The main functional groups of the predicted structure can be observed with corresponding infrared adsorption peaks [11]. As shown in Fig. 1(a), the adsorption peaks appearing at 3,080 and 3,022 cm^{-1} were attributed to the asymmetric and symmetric stretching vibration of C–H bond of the benzene ring in polystyrene. The adsorption peak at 2,925 cm^{-1} could be attributed to the asymmetric and symmetric stretching vibration of CH_2. The adsorption peaks at 1,939, 1,871, and 1,804 cm^{-1} were due to the frequency doubling peak of the benzene ring. The strong peaks around 1,600 and 1,450 cm^{-1} were attributed to the asymmetric and symmetric stretching vibration of C–C=C. As shown in Fig. 1(b), the adsorption peaks which appeared at 1,175 and 1,130 cm^{-1} were attributed to the asymmetric and symmetric stretching vibration of S=O group. As compared to Fig. 1(a), the characteristic adsorption peak of the polystyrene originally appearing at 1,015 cm^{-1} was divided into two peaks at 1,035 and 1,005 cm^{-1}, respectively, and the adsorption peaks at 1,950 and 1,700 cm^{-1} disappeared when the polystyrene was added after sulfonation. The results revealed that the sulfonic group was successfully introduced into the molecular chain of polystyrene [24].

The X-ray diffraction (XRD) patterns of Fe_3O_4 and St-DVB magnetic porous microspheres are shown in Fig. 2. Six XRD diffraction peaks appearing at 2θ = 30.08, 35.49, 42.97, 53.21, 56.90, and 62.54 were indexed to (2 2 0), (3 1 1), (4 0 0), (4 2 2), (5 1 1), and (4 4 0) planes of Fe_3O_4 (JCPDS 39-1346) [25]. The XRD diffraction pattern of St-DVB magnetic porous microspheres was similar to that of Fe_3O_4. The strength of XRD diffraction peaks of St-DVB magnetic porous microspheres was slightly lower than that of Fe_3O_4, which could be attributed to the cover of polymer.

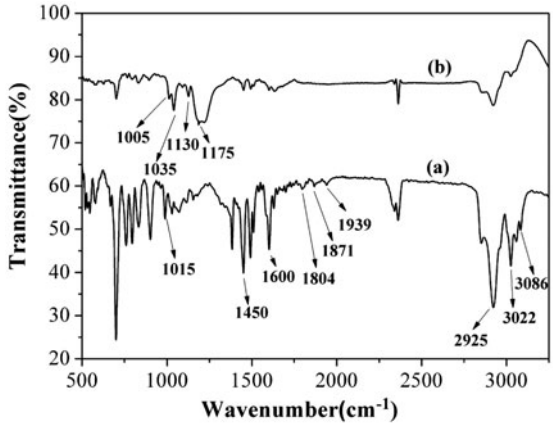

Fig. 1. FT-IR spectra of St-DVB porous microspheres (a) and St-DVB magnetic porous microspheres (b).

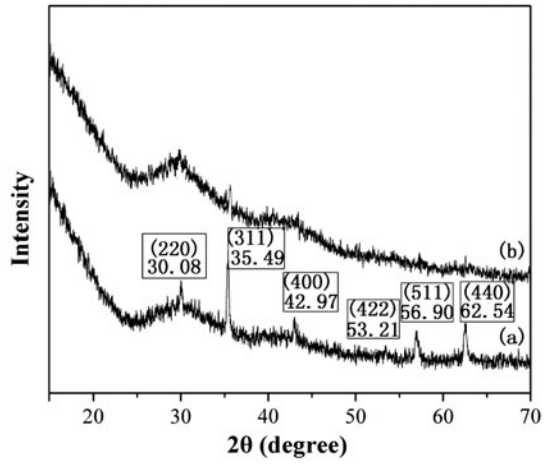

Fig. 2. XRD patterns of Fe_3O_4 (a) and St-DVB magnetic porous microspheres (b).

The results showed that the internal magnetic material in the St-DVB magnetic porous microspheres was Fe_3O_4. The introduction of Fe_3O_4 into St-DVB porous microspheres did not change the crystal structure of Fe_3O_4.

Fig. 3 showed the SEM images of the as-prepared and spent St-DVB microspheres. As shown in Fig. 3(a), the as-prepared St-DVB particulates were spherical microparticles with the average particle sizes of 7 μm. The amplified SEM image (Fig. 3(b)) clearly shows that the surfaces of St-DVB microspheres were porous with a number of cavities. Fig. 3(c) shows the morphology of the spent St-DVB microspheres after recycle for 3 times. The surfaces of the spent St-DVB microspheres appeared leading to a peeling phenomenon due to the effect of eluent with acidity, but as can be seen from Fig. 3(d), the surfaces of the microspheres still had many cavities, which ensured that the spent St-DVB microspheres still had good adsorption performance. Furthermore, the surface energy spectrum diagram is shown in Fig. 3(e). It further confirmed the presence of the magnetic materials in the microspheres.

The magnetic hysteresis loop of the magnetic porous microspheres was recorded by VSM at room temperature. As shown in Fig. 4(a), the general shape and trend of the curve indicated that the St-DVB microspheres were super paramagnetic [26]. The magnetic saturation value of the microspheres was 40 emu g^{-1}, showing that the microspheres had strong magnetic responsiveness. Fig. 4(b) shows that the magnetic properties of the microspheres and magnetic microspheres hybrid solution could be effectively separated by an external magnetic field. Fig. 4(c) shows that the magnetic leakage of the magnetic porous microspheres was weak. The results showed that the magnetic microspheres were stable.

The TGA and DTA profiles of the St-DVB magnetic porous microspheres are shown in Fig. 5. It was obvious that the TGA profile exhibited a weight loss of *ca.* 8%, accompanied with an endothermic peak around 100˚C in the DTA profile due to the evaporation of water molecules. An exothermic peak ranging from 450 to 500˚C was shown in DTA profile, which was accompanied with obvious weight loss in TGA profile due to the rapid polymer decomposition. When the temperature was higher than 800˚C, no obvious weight loss was observed. The results showed that the magnetic content in the ST-DVB magnetic porous microspheres was *ca.* 40%.

The specific surface area and porous properties of St-DVB microspheres were investigated using the N_2 adsorption–desorption measurement. Fig. 6(a) shows

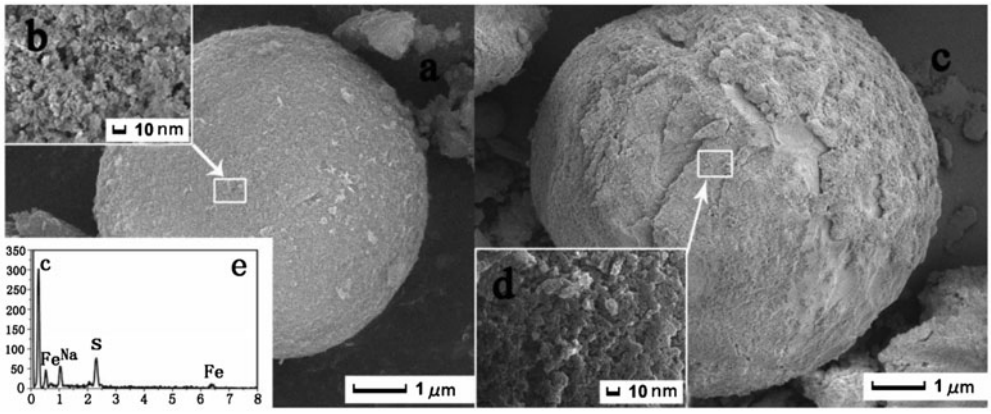

Fig. 3. SEM images of St-DVB microspheres (a), surface detail (b), microspheres after regeneration (c), surface detail (d), and energy spectrum diagram (e).

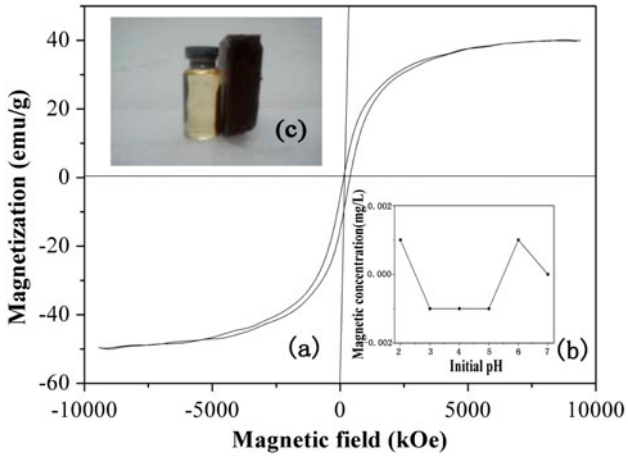

Fig. 4. Magnetization curve of St-DVB microspheres (a), curve of magnetic leakage (b), and photographs of microspheres suspended in the presence of an externally placed magnet (c).

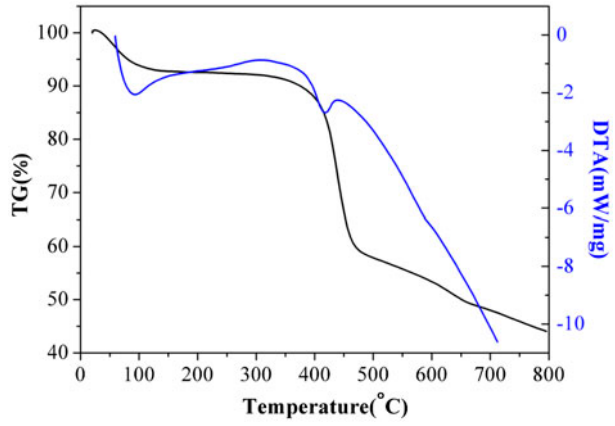

Fig. 5. TG/DTA curve of St-DVB microspheres.

the N_2 adsorption–desorption isotherm of the St-DVB porous magnetic microspheres. The specific surface area of St-DVB porous magnetic microspheres was *ca.* 429 $m^2 g^{-1}$. According to the Brunauer-Deming-Deming-Teller (BDDT) classification method, the isotherm can be grouped into type Ⅱ [27]. As shown in Fig. 6(a), the isotherm possessed hysteresis loop, and the sharp increase in the N_2-adsorbed quantity near the relative pressure of 1 indicated the presence of macrospores [28]. The porous size distribution is shown in Fig. 6(b). The calculated pore diameter of the St-DVB porous magnetic microspheres was *ca.* 6.6 nm.

3.2. Effect of pH

It is well known that the pH can affect the adsorption performance, which plays a key factor in the adsorption process. The pH of solution affects the degree of ionization, which subsequently leads to a change in reaction equilibrium and kinetics characteristics of the adsorption process [29]. In the present investigation, the adsorption of 2,4-DCP and 2,4,6-TCP on magnetic porous microspheres was studied at different initial pHs between 2.0 and 8.0. In Fig. 7(a), it is observed that the adsorption capacity for 2,4-DCP and 2,4,6-TCP was decreased with the increase of pH value from 2.0 to 8.0. The peak of the adsorption performance appeared at pH 2.0 and 3.0 for 2,4-DCP and 2,4,6-TCP, respectively. It can be explained that hydrophobic interaction is the main interaction between adsorbate and adsorbent at low pH and dissociated dichlorophenol molecules may decrease the adsorption capacity at a higher pH [12]. Fig. 7(a) also illustrates that the adsorption capacity of 2,4-DCP was quite higher than that of 2,4,6-TCP. The reason may be that 2,4,6-TCP has one more chlorine functional group than 2,4-DCP, which may increase the resistance with hydrogen bonding and subsequently form space steric hindrance. As a result, the magnetic porous microspheres showed excellent adsorption performance for 2,4-DCP in the pH range between 2.0 and 8.0.

3.3. Adsorption isotherm

The adsorption capacity of the adsorbents and adsorption process can be well described by adsorption isotherm model. In the present investigation, the equilibrium data of adsorption 2,4-DCP and 2,4,6-TCP were fitted to the Langmuir and Freundlich isotherm equation [30]. The correlation coefficient (R^2) was used to judging the applicability of the isotherm models to the adsorption behaviors. Fig. 8 illustrates the comparison of Langmuir and Freundlich isotherm models for 2,4-DCP and 2,4,6-TCP adsorption onto magnetic porous microspheres. The adsorption isotherm constants are summarized in Table 1. The Langmuir equation can be expressed as linear and non-linear forms by Eqs. (2) and (3), respectively.

$$\frac{C_e}{Q_e} = \frac{1}{Q_m K_L} + \frac{C_e}{Q_m} \tag{2}$$

$$Q_e = \frac{K_L Q_m C_e}{1 + K_L C_e} \tag{3}$$

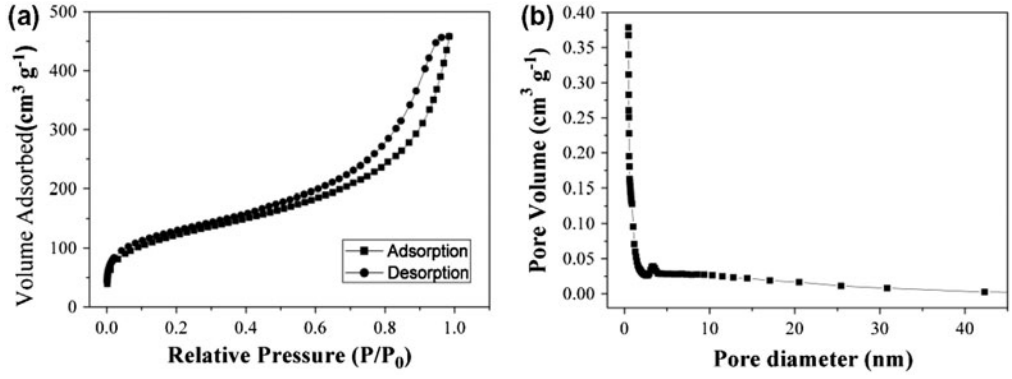

Fig. 6. Nitrogen adsorption–desorption isotherm (a) and the corresponding pore size distribution curve (b).

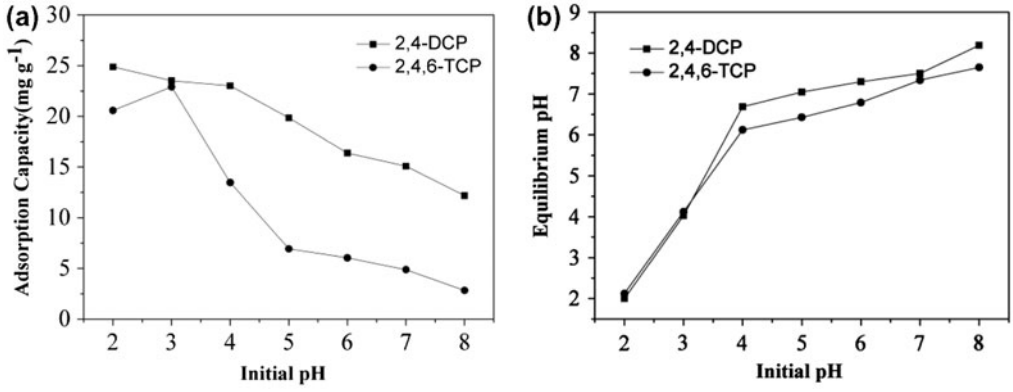

Fig. 7. Effect of pH on adsorption of 2,4-DCP and 2,4,6-TCP (a) and effect of initial pH on equilibrium pH (b).

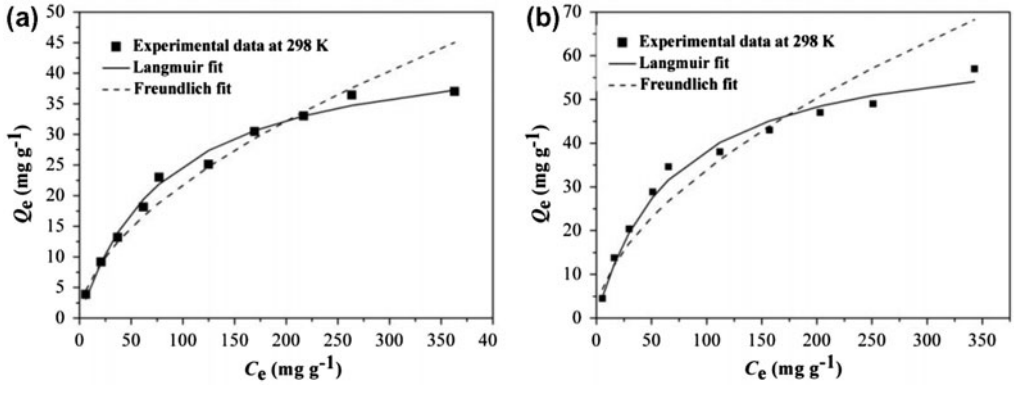

Fig. 8. Comparison of Langmuir and Freundlich isotherm models for 2,4-DCP adsorption onto microspheres (a) and 2,4,6-TCP adsorption onto microspheres (b).

where C_e is the equilibrium concentration of St-DVB magnetic porous microspheres (mg L^{-1}), Q_m (mg g^{-1}) is the maximum adsorption capacity, Q_e is the equilibrium adsorption capacity (mg g^{-1}), and K_L represents the affinity constant.

For predicting the favorability of an adsorption system, the Langmuir equation can also be expressed in terms of a dimensionless separation factor R_L (4) defined as follows [29].

Table 1
Adsorption isotherm constants for 2,4-DCP and 2,4,6-TCP onto microspheres at 298 K. Sorbent dose: 10.0 mg, solution volume: 10.0 mL, solution pH: 2.0 for 2,4-DCP and 3.0 for 2,4,6-TCP, and contact time: 12 h

Adsorption isotherm models	contents	2,4-DCP	2,4,6-TCP
Langmuir equation	R^2	0.991	0.99
	$Q_{m.c}$ (mg g^{-1})	45.872	64.94
	K_L (L mg^{-1})	0.012	0.015
	R_L	0.2	0.147
Freundlich equation	R^2	0.975	0.931
	K_F (mg g^{-1})	1.64	2.523
	n	1.78	1.77

$$R_L = \frac{1}{1 + C_m K_L} \tag{4}$$

where C_m is the maximal initial concentration of the adsorption solution. R_L indicates the favorability and the capacity of adsorption system. When $0 < R_L < 1.0$, it represents good adsorption.

The Freundlich isotherm equation can be expressed as linear and non-linear forms by Eqs. (5) and (6), respectively.

$$\ln Q_e = \ln K_F + \left(\frac{1}{n}\right) \ln C_e \tag{5}$$

$$Q_e = K_F C e^{1/n} \tag{6}$$

where K_F (mg g^{-1}) and n are the Freundlich model constants related to the capacity and intensity of the adsorption, respectively. The value of $1/n$ ranging from 0.1 to 1.0 represents a favorable adsorption condition.

Fig. 8 shows that with the increase of solution concentration from 10 to 400 mg L^{-1}, the adsorption capacity (Q_e) for 2,4-DCP and 2,4,6-TCP onto magnetic porous microspheres was increased sharply at first, then increased slightly, and finally reached to equilibrium. The experimental data were fitted to both Langmuir and Freundlich isotherm equations. Compared with Freundlich isotherm model, the experimental data was more suitable for Langmuir isotherm model. The Q_e of 2,4-DCP and 2,4,6-TCP at 298 K was 38 and 50 mg g^{-1}, respectively. Compared to the previous literature [11,12], the maximum adsorption capacity of magnetic porous microspheres in our work is much higher than other adsorbents, showing the favorable performance of the magnetic polymer materials in our work. Moreover, Fig. 8 also indicated that the adsorption capacity for 2,4,6-TCP on microspheres was slightly higher than for 2,4-DCP. Table 1 verified the above conclusion. It is obvious that correlation coefficient (R^2) that fitted to the Langmuir isotherm was higher than that of Freundlich isotherm model from Table 1.

3.4. Adsorption kinetics

Generally, the adsorption process involved three steps: external mass transfer, inter particle transport, and chemisorption [31]. In the present investigation, the pseudo-first-order and pseudo-second-order equations were used to analyze the adsorption kinetic data [32]. The pseudo-first-order equation can be expressed as linear and non-linear forms by Eqs. (7) and (8), respectively.

$$\ln(Q_e - Q_t) = \ln Q_e - k_1 t \tag{7}$$

$$Q_t = Q_e - Q_e e^{-k_1 t} \tag{8}$$

The pseudo-second-order equation can be expressed as linear and non-linear forms by Eqs. (9) and (10), respectively.

$$\frac{t}{Q_t} = \frac{1}{K_2 Q_e^2} + \frac{t}{Q_e} \tag{9}$$

$$Q_t = \frac{k_2 Q_e^2 t}{1 + k_2 Q_e t} \tag{10}$$

Where Q_e and Q_t (mg g^{-1}) are the amounts of 2,4-DCP and 2,4,6-TCP adsorbed onto St-DVB magnetic porous microspheres at equilibrium and at various time t (min), respectively. K_1 (min^{-1}) is the equilibrium rate constant of the pseudo-first-order model, and the parameter k_1 can be obtained by plotting ln (Q_e–Q_t) vs. t. K_2 (g mg^{-1} min^{-1}) is the pseudo-second-order

model rate constant and can be calculated from the plot of t/Q_t vs. t [33].

Fig. 9 shows the strong time dependence of the adsorption capacities of 2,4-DCP and 2,4,6-TCP on magnetic porous microspheres. It was observed that the adsorption process could be divided into two steps. In the first step, the adsorption rate was fast, and it took about 250 min for 2,4-DCP and 130 min for 2,4,6-TCP to attain equilibrium, respectively. In the second step, the adsorption process gradually achieved equilibrium [34]. It can be seen from Table 2 that all R^2 values ($R^2 > 0.99$) of this adsorption process on the magnetic porous microspheres by pseudo-second-order kinetic model are higher than that by pseudo-first-order kinetic model [35]. Compared with other reported adsorbents [36], although the equilibrium time was slightly longer than that of the other adsorbents, the adsorption capacity of magnetic porous microspheres was prominent. The microspheres have broad application in wastewater treatment.

3.5. Adsorption thermodynamics

Thermodynamic parameters, such as change in Gibbs free energy ($\otimes G^\circ$), enthalpy (ΔH°), and entropy (ΔS°) were calculated using the following Eqs. (11) and (12) [37].

$$\ln\left(\frac{Q_e}{C_e}\right) = \frac{\Delta S^\circ}{R} - \frac{\Delta H^\circ}{RT} \tag{11}$$

$$\Delta G = \Delta H^\circ - T\Delta S^\circ \tag{12}$$

where R is the gas constant (8.314 J mol^{-1} K^{-1}) and T is the absolute temperature (K). ΔG is the Gibbs free energy, $\Delta H^\circ$and ΔS° are represented enthalpy and entropy, respectively. ΔS° and ΔH° are obtained from the slope and intercept of the line plotted by $\ln(Q_e/C_e)$ vs. $1/t$, respectively. The negative value of ΔG represents the adsorption process is spontaneous. The positive value of ΔH° represents the adsorption process is endothermic.

$\Delta G < 0$ indicated that the adsorption process was spontaneous in Table 3. As 2,4-DCP and 2,4,6-TCP adsorbed onto the surface of adsorbents, along with the number of water molecules in solution decreased, the degrees of freedom of the water molecule was increased. The positive values of entropy change ΔS° suggested increased randomness at the solid solution interface during the adsorption 2,4-DCP and 2,4,6-TCP onto microspheres surface [23]. The enthalpy change $\Delta H^\circ > 0$ suggested that the adsorption process was endothermic. As the temperature increased, the adsorption of 2,4-DCP and 2,4,6-TCP onto magnetic porous microspheres was gradually enhanced.

3.6. Regenerability

Regenerability is a key factor for an effective absorbent. The adsorption capacity of the magnetic porous microspheres adsorbent for 2,4-DCP and 2,4,6-TCP with three consecutive adsorption–regeneration cycles is shown in Fig. 10. At the first adsorption step, the adsorption capacities for 2,4-DCP and 2,4,6-TCP reached the values of 26.2 and 35.1 mg g^{-1}, respectively. It was clearly seen that magnetic porous microspheres could be effectively regenerated for further use with only about 5.9 and 7.3% loss of initial binding capacity after three cycles. The rate of adsorption loss was calculated by Eq. (13).

$$R = \frac{(C_F - C_L)}{C_F} \tag{13}$$

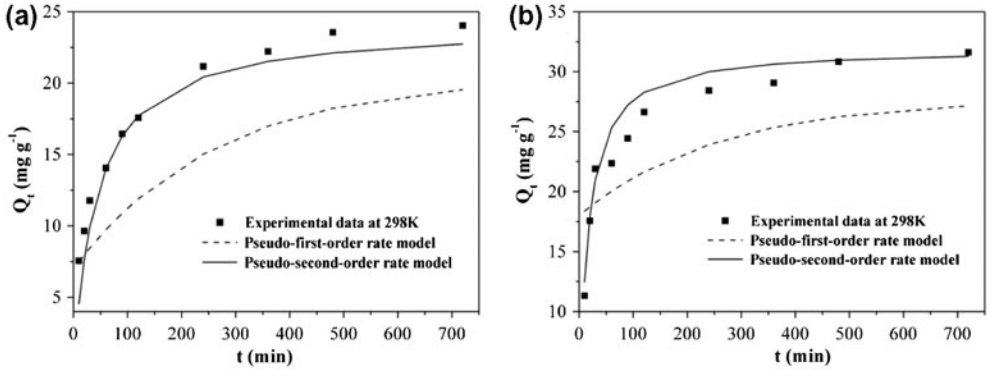

Fig. 9. Comparison of pseudo-first-order and pseudo-second-order kinetic models for 2,4-DCP adsorption onto microspheres (a) and 2,4,6-TCP adsorption onto microspheres (b).

Table 2
Kinetic constants for the pseudo-first-order model and pseudo-second-order model

Pseudo-first-order model							Pseudo-second-order model		
	C_0 (mg L^{-1})	T (K)	$Q_{e,exp}$ (mg g^{-1})	$Q_{e,c}$ (mg g^{-1})	k_1 (L min^{-1})	R^2	$Q_{e,c}$ (mg g^{-1})	k_2 (g mg^{-1} min^{-1})	R^2
2,4-DCP	100	298	24.02	13.41	0.0038	0.8663	24.10	0.001	0.990
2,4,6-TCP	100	298	31.61	9.745	0.0039	0.8985	31.95	0.002	0.998

Table 3
Thermodynamic parameters for the adsorption of 2,4-DCP and 2,4,6-TCP onto microspheres. Sorbent dose: 10.0 mg, solution volume: 10.0 mL, solution pH: 2.0 for 2,4-DCP and 3.0 for 2,4,6-TCP, contact time: 12 h, and reaction temperature is 298, 308 and 318 K, respectively

		Thermodynamic parameters		
Phenol	Temperature (K)	ΔG (kJ mol^{-1})	ΔH (kJ mol^{-1})	ΔS (J mol^{-1} k^{-1})
2,4-DCP	298	−5.97	6.65	20.78
	308	−6.18		
	318	−6.39		
2,4,6-TCP	298	−6.94	4.16	24.11
	308	–7.18		
	318	–7.42		

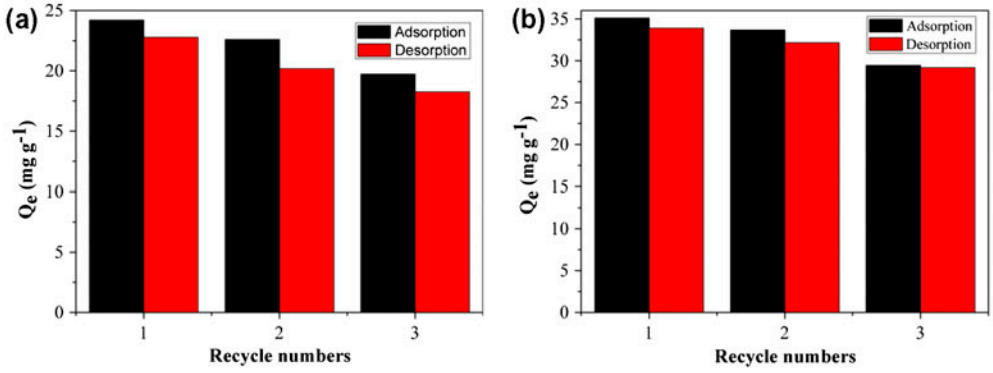

Fig. 10. Recycling of the adsorption and desorption at 298 K methanol:acetic acid (V:V)=100:10 as the eluent.

where C_F is the adsorption capacity of the first time and C_L is the adsorption capacity of the last time. The adsorption capacity of microspheres for 2,4-DCP was about 18.47% loss, and 16.1% loss for 2,4,6-TCP. The results indicated that the microspheres with renewable performance.

4. Conclusion

In this study, Styrene-Divinyl benzene porous microspheres were obtained based on suspension polymerization. We adopted sulfuric acid as surface modification agent and then the microspheres were coated with sulfonic acid group; after several times of ion exchange and oxidation process, the resulting magnetic porous microspheres were successfully prepared and evaluated as an adsorbent for the adsorptive removal of 2,4-DCP and 2,4,6-TCP from aqueous solution. The resulting St-DVB magnetic porous microspheres exhibited excellently spherical morphology, saturation magnetization, and thermal stability. The adsorption performance of the St-DVB magnetic

porous microspheres were manifested by batch mode adsorption experiments. The Langmuir isotherm model was fitted to the equilibrium data better than the Freundlich model, The kinetic properties of St-DVB magnetic porous microspheres were well described by the pseudo-second-order equation, and the equilibrium time for 2,4-DCP and 2,4,6-TCP was 250 and 130 min at 298 K, respectively. The Gibbs free energy function showed that the adsorption process was spontaneous and endothermic. Moreover, the St-DVB magnetic porous microspheres could be used at least three times without weakening the binding capacity significantly. All the above-mentioned results indicate the potential application of the porous microspheres adsorbents for effective removal of 2,4-DCP and 2,4,6-TCP in water or wastewater treatment.

Acknowledgments

This work was financially supported by the National Natural Science Foundation of China (No. 21176107, No. 21107037), Research Fund for the Doctoral Program of Higher Education of China (No. 20110205110014), Jiangsu Planned Projects for Postdoctoral Research Funds (No. 1102119C), Siping Planned Projects for development of science and technology (No. 2013043, No. 2012042), Natural Science Foundation of Jilin Province (No. 20130101179JC_15), and Science and Technology research Foundation of Jilin Province Department of Education (No. 2014_158)

References

[1] D.Y. Pek, N. Kabay, M. Yüksel, D. Yap, Ü. Yüksel, Application of adsorption-ultrafiltration hybrid method for removal of phenol from water by hypercrosslinked polymer adsorbents, Desalination 306 (2012) 24–28.
[2] L. Damjanović, V. Rakić, V. Rac, D. Stošić, A. Auroux, The investigation of phenol removal from aqueous solutions by zeolites as solid adsorbents, J. Hazard. Mater. 184 (2010) 477–484.
[3] V.C. Srivastava, M.M. Swamy, I.D. Mall, B. Prasad, I.M. Mishra, Adsorptive removal of phenol by bagasse fly ash and activated carbon: Equilibrium, kinetics and thermodynamics, Colloids Surf. A. Eng. Asp. 272 (2006) 89–104.
[4] G. Busca, S. Berardinelli, C. Resini, L. Arrighi, Technologies for the removal of phenol from fluid streams: A short review of recent developments, J. Hazard. Mater. 160 (2008) 265–288.
[5] S. Mukherjee, S. Kumar, A.K. Misra, M. Fan, Removal of phenols from water environment by activated carbon, bagasse, ash and wood charcoal, Chem. Eng. J. 129 (2007) 133–142.
[6] P.A. Deshpande, G. Madras, Photocatalytic degradation of phenol by base metal substituted orthovanadates, Chem. Eng. J. 161 (2010) 136–145.
[7] J.A. Zazo, J.A. Casas, A.F. Mohedano, J.J. Rodriguez, Semicontinuous Fenton oxidation of phenol in aqueous solution. A kinetic study, Water Res. 43 (2009) 4063–4069.
[8] Z. Aleksieva, D. Ivanova, T. Godjevargova, Carbon-coated anatase: Adsorption and decomposition of phenol in water, Process Biochem. 37 (2002) 1215–1219.
[9] T. Vatai, M. Skerget, Z. Knez, Extraction of phenolic compounds from elder berry and different grape marc varieties using organic solvents and/or supercritical carbon dioxide, J. Food Eng. 90 (2009) 246–254.
[10] Y.S. Ng, N.S. Jayakumar, M.A. Hashim, Performance evaluation of organic emulsion liquid membrane on phenol removal, J. Hazard. Mater. 184 (2010) 255–260.
[11] J.M. Pan, H. Yao, X.X. Li, B. Wang, P.W. Huo, W.Z. Xu, H.X. Ou, Y.S. Yan, Synthesis of chitosan/γ-Fe_2O_3/fly-ash-cenospheres composites for the fast removal of bisphenol A and 2,4,6-trichlorophenol from aqueous solutions, J. Hazard. Mater. 190 (2011) 276–284.
[12] J.M. Pan, X.H. Zou, X. Wang, W. Guan, C.X. Li, Y.S. Yan, X.Y. Wu, Adsorptive removal of 2,4-didichlorophenol and 2,6-didichlorophenol from aqueous solution by β-cyclodextrin/attapulgite composites: Equilibrium, kinetics and thermodynamics, Chem. Eng. J. 166 (2011) 40–48.
[13] M.S. Islam, J.H. Yeum, A.K. Das, Synthesis of poly (vinyl acetate–methyl methacrylate) copolymer microspheres using suspension polymerization, J. Colloid Interface Sci. 368 (2012) 400–405.
[14] D. Horak, E. Pollert, M. Trchova, J. Kovarova, Magnetic poly (glycidyl methacrylate)-based microspheres prepared by suspension polymerization in the presence of modified $La0.75Sr0.25MnO_3$ nanoparticles, Eur. Polym. J. 45 (2009) 1009–1016.
[15] N.S. Kwak, Y. Baek, T.S. Hwang, The synthesis of poly(vinylphosphonic acid-co-methacrylic acid) microbeads by suspension polymerization and the characterization of their indium adsorption properties, J. Hazard. Mater. 203–204 (2012) 213–220.
[16] L.C. Xu, J.D. Dai, J.M. Pan, X.X. Li, P.W. Huo, Y.S. Yan, X.B. Zou, R.X. Zhang, Performance of rattle-type magnetic mesoporous silica spheres in the adsorption of single and binary antibiotics, Chem. Eng. J. 174 (2011) 221–230.
[17] A. Navarro, C. del R´ıo, J.L. Acosta, Kinetic study of the sulfonation of hydrogenated styrene butadiene block copolymer (HSBS) Microstructural and electrical characterizations, J. Membr. Sci. 30 (2007) 79–87.
[18] C.A. Toro, R. Rodrigo, J. Cuellar, Sulfonation of macroporous poly (styrene-co-divinylbenzene) beads: Effect of the proportion of isomers on their cation exchange capacity, React. Funct. Polym. 68 (2008) 1325–1336.
[19] P. Ergenekon, E. Gürbulak, B. Keskinler, A novel method for sulfonation of microporous polystyrene divinyl benzene copolymer using gaseous SO_2 in the waste air streams, Chem. Eng. Process 50 (2011) 16–21.
[20] L. Li, J. Cheng, X.F. Wen, Synthesis and characterization of suspension polymerized styrene-divinylbenzene porous microsphere using as slow-release-active carrier, Chin. J. Chem. Eng. 14(4) (2006) 471–477.

[21] Y.L. Tai, L. Wang, J.M. Gao, Synthesis of Fe_3O_4@poly (methylmethacrylate-co-divinylbenzene) magnetic porous microspheres and their application in the separation of phenol from aqueous solutions, J. Colloid Interface Sci. 360 (2011) 731–738.
[22] L.C. Xu, J.M. Pan, J.D. Dai, Z.J. Cao, H. Hang, X.X. Li, Y.S. Yan, Magnetic ZnO surface-imprinted polymers prepared by ARGET ATRP and the application for antibiotics selective recognition, RSC Adv. 2 (2012) 5571–5579.
[23] J.M. Pan, X.H. Zou, X. Wang, W. Guan, Y.S. Yan, J. Han, Selective recognition of 2,4-dichlorophenol from aqueous solution by uniformly sized molecularly imprinted microspheres with β-cyclodextrin/attapulgite composites as support, Chem. Eng. J. 162 (2010) 910–918.
[24] X. Lu, R.A. Weiss, Specific inteactions and ionic aggregation in miscible blends of nylon-6 and zinc sulfonated polystyrene ionomer, Macromolecules 25(23) (1992) 6185–6189.
[25] H.Y. Zhu, R. Jiang, L. Xiao, W. Li, A novel magnetically separable Fe_2O_3/crosslinked chitosan adsorbent: Preparation, characterization and adsorption application for removal of hazardous azo dye, J. Hazard. Mater. 179 (2010) 251–257.
[26] X. Wang, L.Y. Wang, X.W. He, Y.K. Zhang, L.X. Chen, A molecularly imprinted polymer-coated nanocomposite of magnetic nanoparticles for estrone recognition, Talanta 78 (2009) 327–332.
[27] W.D. Shi, Y. Yan, Y. Yan, Microwave-assisted synthesis of nano-scale $BiVO_4$ photocatalysts and their excellent visible-light-driven photocatalytic activity for the degradation of ciprofloxacin, Chem. Eng. J. 215–216 (2013) 740–746.
[28] D. Liu, P. Yuan, D.Y. Tan, H.M. Liu, T. Wang, M.D. Fan, J.X. Zhu, Facile preparation of hierarchically porous carbon using diatomite as both template and catalyst and methylene blue adsorption of carbon products, J. Colloid Interface Sci. 388 (2012) 176–184.
[29] N.S. Kumar, M. Suguna, M.V. Subbaiah, A.S. Reddy, N.P. Kumar, A. Krishnaiah, Adsorption of phenolic Compounds from aqueous solutions onto chitosan-coated perlite beads as biosorbent, Ind. Eng. Chem. Res. 49 (2010) 9238–9247.
[30] F.Q. An, R.K. Du, X.H. Wang, M. Wan, X. Dai, J.F. Gao, Adsorption of phenolic compounds from aqueous solution using salicylic acid type adsorbent, J. Hazard. Mater. 201–202 (2012) 74–81.
[31] W.S. Wang, B.C. Zheng, Z.L. Deng, Z.J. Feng, L.F. Fu, Kinetics and equilibriums for adsorption of poly(vinyl alcohol) from aqueous solution onto natural bentonite, Chem. Eng. J. 214 (2013) 343–354.
[32] Y.W. Chen, R.M. Cheng, X.C. Xu, Study the adsorption of phenol from aqueous solution on hydroxyapatite nanopowders, J. Hazard. Mater. 161 (2009) 231–240.
[33] N. Kannan, M.M. Sundaram, Kinetics and mechanism of removal of methylene blue by adsorption on various carbons-a comparative study, Dyes Pigm. 51 (2001) 25–40.
[34] Y. Li, X. Li, Y.Q. Li, J.Y. Qi, J. Bian, Y.X. Yuan, Selective removal of 2,4-dichlorophenol from contaminated water using non-covalent imprinted microspheres, Environ. Pollut. 157 (2009) 1879–1885.
[35] G. Baydenmir, M. Andac, N. Bereli, R. Say, A. Denizli, Selective removal of bilirubin from human plasma with bilirubin-imprinted particles, Ind. Eng. Chem. Res. 46 (2007) 2843–2852.
[36] M. Sathishkumar, A.R. Binupriya, D. Kavitha, R. Selvakumar, R. Jayabalan, J.G. Choi, S.E. Yun, Adsorption potential of maize cob carbon for 2,4-dichlorophenol removal from aqueous solutions: Equilibrium, kinetics and thermodynamics modeling, Chem. Eng. J. 147 (2009) 265–271.
[37] A. Mellah, S. Chegrouche, M. Barkat, The removal of uranium (VI) from aqueous solutions onto activated carbon: kinetic and thermodynamic investigations, J. Colloid Interface Sci. 296 (2006) 434–441.